

Influence of Size and Location of a Thin Baffle on Natural Convection in a Vertical Annular Enclosure

M. Sankar^{1†}, B. V. Pushpa², B. M. R. Prasanna³ and Y. Do⁴

¹ *Department of Mathematics, School of Engineering, Presidency University, Bangalore, India*

² *Department of Mathematics, Sapthagiri college of Engineering, Bangalore, India*

³ *Department of Mathematics, Siddaganga Institute of Technology, Tumkur, India*

⁴ *Department of Mathematics, KNU-Center for Nonlinear Dynamics, Kyungpook National University, Daegu, South Korea*

†Corresponding Author Email: manisankarir@yahoo.com

(Received August 14, 2015; accepted January 24, 2016)

ABSTRACT

This article reports the numerical study of natural convection in a differentially heated cylindrical annular enclosure with a thin baffle attached to inner wall. The inner and outer walls of the annulus are respectively maintained at higher and lower temperatures, whereas the top and bottom walls are thermally insulated. Using an implicit finite difference technique, the effects of baffle size and location on natural convection has been investigated for different Rayleigh numbers and radius ratios by fixing the Prandtl number at 0.707. Through the detailed numerical simulations, we have successfully captured the important effects of baffle size and location on the flow pattern and heat transfer rate. It has been found that the size and location of baffle modify the flow pattern and heat transfer rate in a completely different conducts. The numerical results corroborates that the average heat transfer rate increases with the Rayleigh number, radius ratio, baffle position; but decreases with baffle length. Further, it has been observed that it is possible to enhance or suppress the flow circulation and heat transfer rates by a proper choice of baffle size and location, and Rayleigh number.

Keywords: Convection; Baffle; Annulus; Finite difference method.

NOMENCLATURE

A	aspect ratio	(r_i, r_o)	radius of inner and outer cylinders
D	width of the annulus	(r, z)	dimensional radial and axial co-ordinates
g	acceleration due to gravity	(R, Z)	dimensionless radial and axial co-ordinates
H	height of the annulus	(u, w)	dimensional velocity in (r, z) directions
h	dimensional position of baffle	α	thermal diffusivity
k	thermal conductivity	β	volume expansion coefficient
l	dimensional length of baffle	ε	dimensionless length of baffle
L	dimensionless position of baffle	ζ	dimensionless vorticity
Nu_L	local Nusselt number at inner wall	θ	dimensional temperature
Nu_R	local Nusselt number at outer wall	λ	radius ratio
\overline{Nu}	average Nusselt number	ν	kinematic viscosity
p	fluid pressure	ρ	fluid density
Pr	Prandtl number	ψ	dimensionless stream function
Ra	Rayleigh number		
T	dimensionless temperature		
t^*	dimensional time		
t	dimensionless time		
(U, W)	dimensionless velocity in (R, Z) directions		
		Subscripts	
		c	cold wall
		h	hot wall

1. INTRODUCTION

Convection heat transfer is an important phenomenon in wide range of applications such as electronic cooling, heat exchangers, cooling of radioactive waste containers and nuclear reactors. Natural convection in an enclosure with two adiabatic horizontal walls, and differentially heated side walls is an important model problem in many industrial applications, which has been investigated in the literature to a great extent (Ostrach 1988, Kumar and Singh 2013, Patil *et al.* 2013, Sankar *et al.* 2014, and Bhattacharya and Das 2015). The enhancement or suppression of heat transfer performance in many industrial applications is essential from the energy saving perspective. In a differentially heated cavity, it was proven through numerical simulations and experimental visualizations that the heat transfer rate is highly sensitive to the flow pattern in different flow regimes. Thus, the heat transfer rate could be controlled effectively if natural convection flow regimes can be manipulated through some mechanism. Among the available techniques, a simple way to alter the flow regimes in a cavity is by introducing baffles or fins attached to the heated or cooled wall. Theoretical and experimental investigations of this phenomenon have been extensively reported in the literature until recently. The effect of length and position of baffle(s) on the flow and heat transfer is significant, since these geometrical parameters play an important role in augmenting or suppressing the convective flow and heat transfer rate. A combined numerical and experimental investigation of conjugate natural convection heat transfer with discrete heat sources and a baffle is examined by Sun and Emery (1997).

Shi and Khodadadi (2003) discussed the influence of location and size of an isothermal fin placed on the hot wall of a rectangular enclosure. They found that the flow patterns are modified by the hydrodynamic blockage effect caused by the fin, and also the fin acts as an extra heating to the fluid. Laminar convective heat transfer in a square cavity with a baffle attached to the hot wall has been numerically investigated by Tasnim and Collins (2004) and found that the presence of baffle on the hot wall increases the heat transfer rate at higher Rayleigh numbers. Later, Oztop *et al.* (2004) examined the effect of natural convection heat transfer in a square enclosure with horizontal and vertical hot plate. Bilgen (2005) carried out a numerical investigation of free convection heat transfer in differentially heated square cavities with a thin fin attached to the hot wall. By considering different relative conductivity of the fin, it has been found that the heat transfer rate increases with Rayleigh number, but decreases with fin length and conductivity ratio. Ben-Nakhi and Chamkha (2006) numerically investigated the effect of an inclined thin fin on natural convection heat transfer in a square enclosure. Recently, Liu *et al.* (2014) investigated natural convection in a differentially heated cavity with two horizontal adiabatic fins on each sidewall. The experimental results have been

visualized by the shadowgraph technique and are in good agreement with their numerical simulations.

Owing to the fundamental importance of complex natural convection phenomena arising in various technological applications, such as thermal insulation, solar-collector design, and fire protection, interest in the study of natural convection in partially or fully divided enclosures has increased in recent years. The position, height and number of partitions, and spacing between the partitions plays a vital role in altering the fluid flow and heat transfer rate in the enclosure. Using finite element method, Nag *et al.* (1994) investigated the effect of a partial horizontal partition of finite thickness, attached to the heated wall of square cavity. They found that the flow field and heat transfer rate can be effectively controlled through the thickness of partition. Natural convection in a partially divided, rectangular enclosure has been numerically studied by Bilgen (2002) by considering one or two conducting partitions. It has been found that the flow regime turn out to be turbulent for $Ra > 10^8$ and the heat transfer rate could be reduced by the location and number of partitions. Natural convection in an inclined enclosure with partitions of different heights has been analyzed by Ben Nakhi and Chamkha (2006). From the numerical results, they concluded that the heat transfer rate and flow pattern are strongly influenced by the dimensionless partition height and inclination angle of the enclosure. To achieve an optimum heat transfer rate in practical engineering applications such as solar collectors or heat exchangers, different shaped duct constructions have also been used. In these applications, the control of fluid flow and heat transfer is an important issue and this has been successfully accomplished by attaching a thin baffle to the hot or cold wall (Tandiroglu 2006, Moukalled and Darwish 2007, Varol and Oztop 2009, and Bose *et al.*, 2013). In addition to the length and location of baffle, the shape of the baffle has also significant influence on the control of fluid flow and heat transfer. It has been found that the shape of baffles attached to the enclosure wall can modulate the flow, cause the re-development of the boundary layers to generate secondary flows, which in turn improve fluid mixing and enhances heat transfer (Tasnim and Collins 2005, and Changzheng *et al.* 2011).

It is apparent from the detailed review of early studies that the effects of a thin baffle on the natural convection heat transfer in a vertical annular enclosure remain unclear, and there is a need for further study in this area. The existing studies on the control of fluid flow and the corresponding heat transfer with the help of baffle(s) mainly deal with rectangular or triangular or trapezoidal or horizontal annular enclosures. To the best of author's knowledge, the effect of baffle on natural convection has been investigated in a vertical annulus by Al-Abidi *et al.* (2013). But, this study mainly concentrates on the solidification of a phase change material (PCM) and close-contact melting

(CCM) suitable for latent heat thermal energy storage. However, the presence of a baffle significantly modifies the flow pattern and heat transfer rate in the annulus, and this aspect has not been discussed by Al-Abidi *et al.* (2013) in the similar geometry. The lack of information on natural convective heat transfer in a vertical annulus with a thin baffle of different lengths and placed at different locations motivates the present investigation. Therefore, the main objective of this investigation is to analyze the size and location effects of a thin baffle on the flow and heat transfer phenomena in a vertical annulus of unit aspect ratio. This problem has important applications in tubular heat exchangers and thermal energy storage systems. The theoretical analysis and the computational simulations are restricted to two-dimensional, axisymmetric flows. In the following section, the physical model and the mathematical formulation are provided. In Section 3, the numerical technique used to solve the governing equations is described. The influence of size and location of a thin baffle on the flow and heat transfer characteristics in the annulus is discussed in Section 4. Finally, the concluding remarks are provided in Section 5.

2. MATHEMATICAL FORMULATION

Consider the vertical annulus formed by two vertical concentric cylinders of inner and outer radii r_i and r_o respectively as shown in Fig. 1a. The width of the annulus is D and height is denoted as H . The cylindrical coordinates (r, z) with the corresponding velocity components (u, w) are also specified in Fig. 1a. In the present study, the flow is considered to be two-dimensional, axisymmetric and the aspect ratio of the annulus has been taken as unity ($H = D$) as shown in Fig. 1b. The top and bottom walls of the annulus are thermally insulated, whereas the inner (left) wall is maintained at a higher temperature (θ_h) and the outer (right) wall is maintained at a lower temperature (θ_c), with $\theta_h > \theta_c$. A horizontal baffle with length l is attached to different locations h on the inner wall. It is assumed that the baffle is made of highly conductive materials and temperature of the baffle is maintained at the same temperature of the inner hot wall. Further, the flow is assumed to be laminar and thermophysical properties of the fluid are taken as constant. The buoyancy effect in the momentum equation is taken through the classical Boussinesq approximation. Accordingly, the density of fluid is assumed to be uniform except in gravitational term, where it is taken as a function of temperature. Also, the fluid is assumed to be Newtonian with negligible viscous dissipation and gravity acts in negative z -direction, and no-slip conditions apply on all boundaries. By employing the above approximations, the dimensionless governing equations in terms of vorticity-stream function equation form are (Sankar *et al.*, 2012 and 2014):

$$\frac{\partial T}{\partial t} + U \frac{\partial T}{\partial R} + W \frac{\partial T}{\partial Z} = \nabla^2 T \quad (1)$$

$$\frac{\partial \zeta}{\partial t} + U \frac{\partial \zeta}{\partial R} + W \frac{\partial \zeta}{\partial Z} - \frac{U\zeta}{R} = Pr \left[\nabla^2 \zeta - \frac{\zeta}{R^2} \right] - PrRa \frac{\partial T}{\partial R} \quad (2)$$

$$\zeta = \frac{1}{R} \left[\frac{\partial^2 \psi}{\partial R^2} - \frac{1}{R} \frac{\partial \psi}{\partial R} + \frac{\partial^2 \psi}{\partial Z^2} \right] \quad (3)$$

$$U = \frac{1}{R} \frac{\partial \psi}{\partial Z}, \quad W = -\frac{1}{R} \frac{\partial \psi}{\partial R}, \quad (4)$$

$$\text{where } \nabla^2 = \frac{\partial^2}{\partial R^2} + \frac{1}{R} \frac{\partial}{\partial R} + \frac{\partial^2}{\partial Z^2}$$

For transforming the present model equations to the above dimensionless form, the following dimensionless variables are defined:

$$(R, Z) = (r, z) / D, (U, W) = (u, w) / (\alpha / D),$$

$$t = t^* / (D^2 / \alpha), T = (\theta - \theta_c) / \Delta \theta$$

$$P = p / (\rho_0 \alpha^2 / D^2), \zeta = \zeta^* / (\alpha / D^2),$$

$$\psi = \psi^* / (D\alpha), \text{ where } D = r_o - r_i, \Delta \theta = \theta_h - \theta_c$$

The present study involves six non-dimensional parameters; two physical parameters (Ra and Pr) and four geometrical parameters (A, λ, ε and L). They are:

$$Ra = \frac{g\beta(\theta_h - \theta_c)D^3}{\nu\alpha}, \text{ the Rayleigh number,}$$

$$Pr = \frac{\nu}{\alpha}, \text{ the Prandtl number, } A = \frac{H}{D}, \text{ the aspect}$$

$$\text{ratio, } \lambda = \frac{r_o}{r_i}, \text{ the radius ratio, } \varepsilon = \frac{l}{H}, \text{ length of}$$

$$\text{the baffle and } L = \frac{h}{H}, \text{ location of the baffle.}$$

The initial and boundary conditions in non-dimensional form are:

$$t = 0: U = W = T = 0, \psi = \zeta = 0;$$

$$\text{for } \frac{1}{\lambda - 1} \leq R \leq \frac{\lambda}{\lambda - 1}, 0 \leq Z \leq A$$

$$t > 0: \psi = \frac{\partial \psi}{\partial R} = 0, T = 1;$$

$$\text{for } R = \frac{1}{\lambda - 1} \text{ and } 0 \leq Z \leq A$$

$$\psi = \frac{\partial \psi}{\partial R} = 0, T = 0;$$

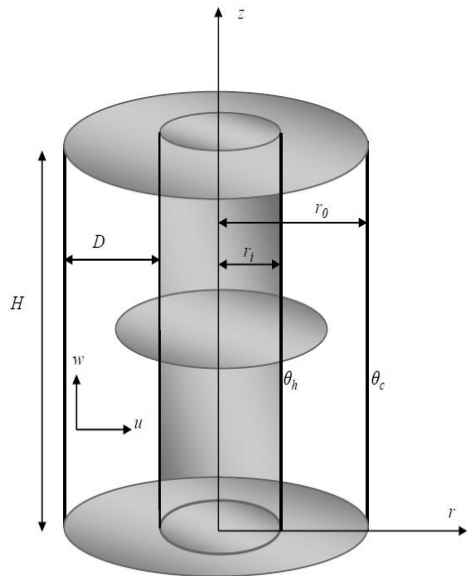
$$\text{for } R = \frac{\lambda}{\lambda - 1} \text{ and } 0 \leq Z \leq A$$

$$\psi = \frac{\partial \psi}{\partial Z} = 0, \frac{\partial T}{\partial Z} = 0; Z = 0 \text{ and } Z = A$$

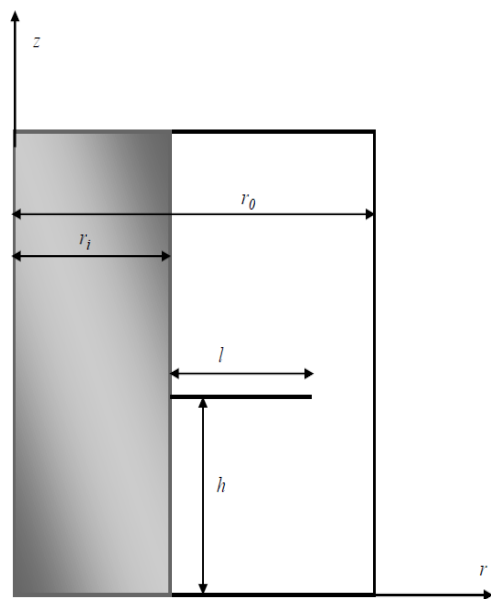
$$\psi = \frac{\partial \psi}{\partial Z} = 0, T = 1; \text{ on the baffle.}$$

The boundary condition on ζ is required to solve the vorticity transport equation at next time levels.

Using Taylor series expansion of the stream function near the walls, this can be derived in the following form: $\zeta_b = \frac{8\psi_{b+1} - \psi_{b+2}}{2(\Delta\eta)^2}$, where b denotes a boundary node and $\Delta\eta$ is the spatial interval in the direction normal to the boundary.



(a)



(b)

Fig. 1. (a) Physical configuration, co-ordinate system and (b) axisymmetric view of the annulus.

When the steady state results are obtained from the unsteady-state Eqs. (1) – (4), the important parameter in heat transfer problems, namely the heat transfer rate has been estimated in terms of local and average Nusselt numbers. The local

Nusselt number is given by $Nu = \frac{hD}{k} = -\frac{\partial T}{\partial R}$. The average Nusselt number is then calculated from the relation $\overline{Nu} = \frac{1}{A} \int_0^A Nu \, dZ$.

3. METHOD OF SOLUTION AND VALIDATION

The time-dependent governing equations and the associated initial and boundary conditions are numerically solved by making necessary changes to the existing code developed by the authors (Sankar *et al.* 2012, Sankar *et al.*, 2013 and Sankar *et al.*, 2014). Also, the modified code has been successfully validated with the standard benchmark solutions. Below, the numerical method is briefly described.

The governing vorticity transport and energy equations are implicitly solved using a stable finite difference technique based on two-step Alternating Direction Implicit (ADI) method. In the governing equations, all second order derivatives and first order linear derivatives are approximated by a second order accurate central differencing scheme. The nonlinear advection terms are discretized using the second upwind difference technique and the time derivative is by forward differencing scheme. Successive Line Over Relaxation (SLOR) method is employed to solve the steady state stream function equation by choosing an optimum relaxation factor. The discretized algebraic equations in tridiagonal structure are solved using the Thomas algorithm. The velocity components are evaluated using central difference approximation to Eq. (4). Finally, the Simpson's rule is applied to evaluate the average Nusselt number. A comprehensive numerical procedure can be found in our recent papers (Sankar *et al.* 2013, 2014).

3.1 Grid Sensitivity Analysis

Prior to the numerical simulations, the results are checked for the grid independency by choosing a uniform grid in the calculation domain. For this, the average Nusselt number (\overline{Nu}) for different grid system in the R and Z directions are obtained. In particular, the grid sizes of 51×51 , 81×81 , 101×101 and 121×121 has been used and an optimum grid size is chosen when \overline{Nu} is unchanged with an increase of grid size. We observed that the maximum difference between 101×101 and 121×121 grid systems is within 0.1%, and hence, for the sake of computational time, a 101×101 grid system is used for further calculations. For brevity, the results pertaining to grid independency are not presented here as the detailed grid independence study can be found in our earlier papers. The steady state solution of the problem has been obtained as an asymptotic limit to the transient solutions. An in-house Fortran code has been developed for the

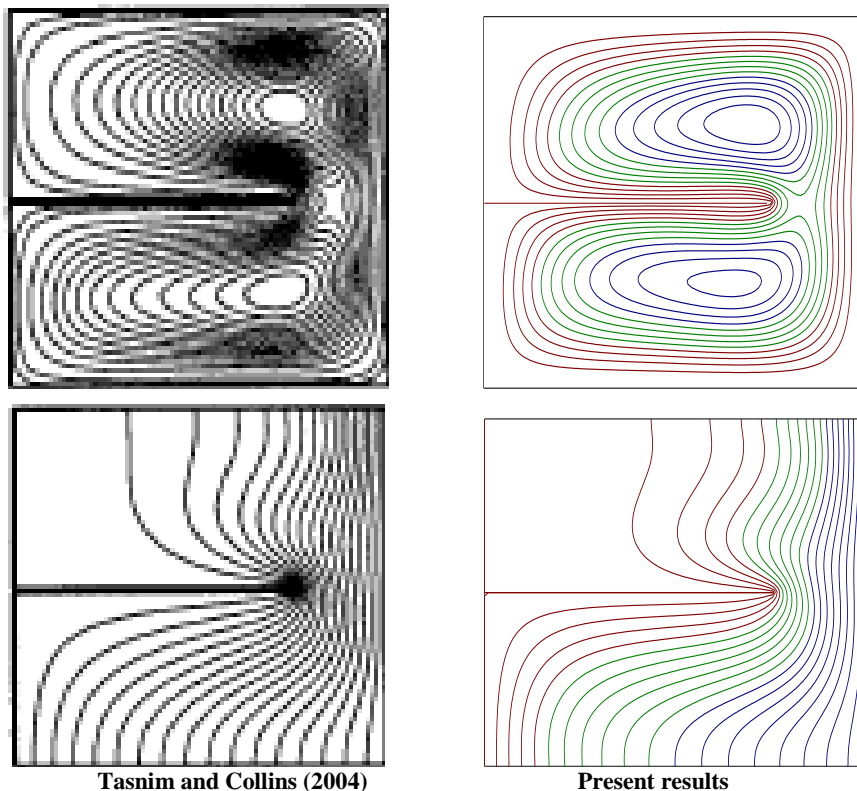


Fig. 2. Comparison of streamlines and isotherms between the numerical results of Tasnim and Collins (2004) and present results for $Ra = 10^4$, $\lambda = 1$, $A = 1$, $L = 0.5$, $\varepsilon = 0.75$ and $Pr = 0.7$.

present model and has been successfully validated against the available benchmark solutions in the literature before performing the simulations, which is discussed in the next section.

3.2 Validation

The numerical procedure used in the present study is the same that has been employed in the recent works by the authors in a vertical annular enclosure (Sankar *et al.* 2011, 2012 and 2014), where we had demonstrated that the numerical results are consistent with the existing benchmark solutions in a discretely as well as uniformly heated porous and nonporous annulus. However, the modified computer code is validated by comparing the present results with the available benchmark results for the limiting case of $\lambda = 1$. When the radius ratio (λ) is unity, the governing equations of the present problem reduces to that of natural convection in a square enclosure with a baffle. For this, the streamlines and isotherms are obtained for $Ra = 10^4$, $\lambda = 1$, $A = 1$, $\varepsilon = 0.5$, $L = 0.75$ and $Pr = 0.7$. Fig. 2 illustrates the comparison of streamlines and isotherms between the present study and that of Tasnim and Collins (2004). From the figure, an overall good degree of agreement can be observed between the present results and the results of Tasnim and Collins (2004). Further, when the baffle length is zero, the average Nusselt numbers measured from the present code are in excellent agreement with the benchmark solutions in annular and rectangular cavities (see Sankar *et al.* 2011,

2012, 2013 and 2014).

4. RESULTS AND DISCUSSION

This section corresponds to the results of numerical simulation to illustrate the influence of size and location of a thin baffle on natural convective flow, thermal fields, and to evaluate the corresponding heat transfer in a vertical annulus. The present study has six non-dimensional parameters; two physical and four geometrical parameters. Since the main aim of this investigation is to analyze the effect of a thin baffle on the convective flow and heat transfer characteristics, we have varied only the main controlling parameters in the simulations. In the present study, the aspect ratio (A) of the annulus and Prandtl number (Pr) are kept fixed respectively at $A=1$ and $Pr = 0.707$. The range of Rayleigh number considered in the present simulation is $10^3 - 10^7$, while the radius ratio (λ) is taken as $1 \leq \lambda \leq 10$. In order to capture the influence of baffle size and location on convective flow and heat transfer rate, we considered the baffle lengths from 25 to 75 percent of the annulus width ($0.25 \leq \varepsilon \leq 0.75$); while the baffle is positioned at five different locations of the inner wall ($0.125 \leq L \leq 0.875$). For the above parameter ranges, the detailed flow fields and temperature distributions are illustrated through streamlines and isotherms in the annular enclosure. In all contour graphs, the left and right vertical sides represent the

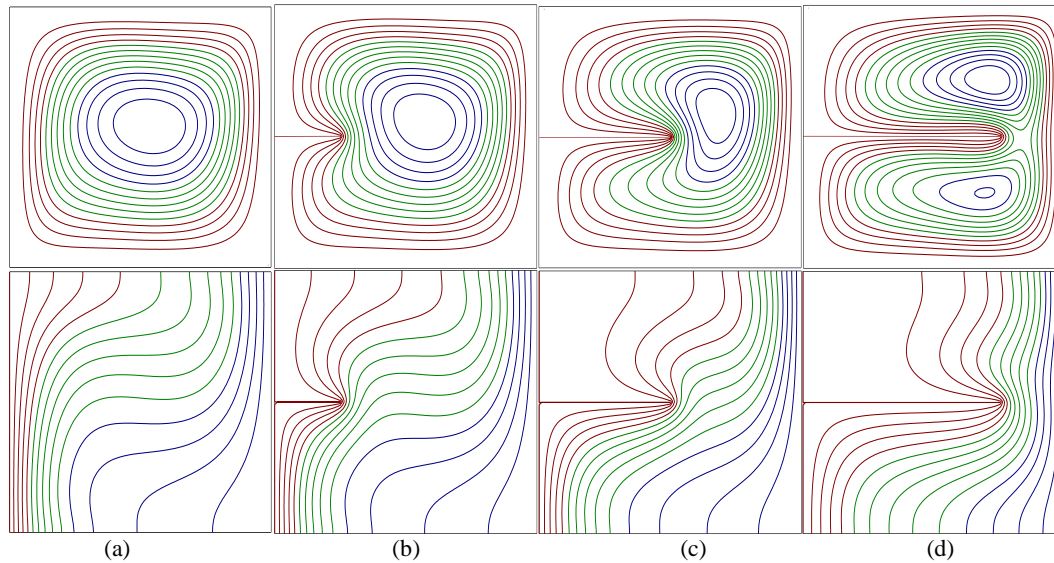


Fig. 3. Effect of baffle length on streamlines (top) and isotherms (bottom) for $L = 0.5$ and $Ra = 10^4$. (a) No baffle, $|\psi_{\max}| = 6.7$, (b) $\varepsilon = 0.25$, $|\psi_{\max}| = 7.4$, (c) $\varepsilon = 0.5$, $|\psi_{\max}| = 6.8$, and (d) $\varepsilon = 0.75$, $|\psi_{\max}| = 3.8$.

inner and outer walls of the annulus respectively. Further, the variation of heat transfer rate is presented in terms of the local and average Nusselt numbers for different combination of Rayleigh numbers, baffle lengths, baffle positions and radius ratios.

4.1 Effect of Baffle Location and Size on Flow and Temperature Fields

To start with the flow simulations, the influence of baffle length on flow and temperature fields are examined by fixing all parameters except baffle length (ε). Specifically, we fix $Ra = 10^4$, $L = 0.5$ and $\lambda = 2$. The streamlines and isotherms are illustrated in Figs. 3 and 4 for different baffle lengths and for two representative values of Rayleigh numbers. Fig. 3 reports the influence of baffle length on the streamlines and isotherms at a lower value of $Ra = 10^4$. In the absence of baffle, the fluid rises due to the heating from inner hot wall, descends along outer cold wall, which causes a clockwise rotating vortex in the middle of the annulus. A similar pattern of thermal fields can be identified from the isotherms. However, as the baffle is positioned at the inner wall, the flow and thermal fields experienced drastic changes qualitatively as well as quantitatively. For smaller baffle length, the outermost streamlines are distorted, and as the baffle length increases, the primary vortex splits into two vortices, and are located above and below the baffle. As the baffle length increases to 75% of the annulus width, the intensity of convective flow drops down due to weak buoyancy force, and is further evident from the appearance of secondary eddy in the annulus. A careful observation of Fig. 3 reveals that the flow circulation rate measured by the magnitude of maximum stream function, $|\psi_{\max}|$, is relatively higher ($|\psi_{\max}| = 7.4$) for smaller baffle length

($\varepsilon = 0.25$). However, as the baffle length is increased ($\varepsilon = 0.5$ and 0.75), the strength of flow circulation decreases significantly ($|\psi_{\max}| = 6.8$ & 3.8). For larger baffle length, the flow strength in the core is much weaker, as can be observed from ($|\psi_{\max}| = 3.8$), and hence the isotherms are also weaker, since the isotherms tend to follow the streamlines. Further examination of isotherms illustrates that the area above the baffle is not completely occupied by the isotherms as baffle length increases, which indicates the existence of stagnant fluid or sluggish movement of fluid flow.

Figure 4 depicts the effect of baffle length for a higher Rayleigh number ($Ra = 10^6$). As expected, the flow circulation rate is increased due to intensified natural convection at higher Rayleigh number. In the absence of baffle, the primary vortex splits into two vortices, and streamlines are denser near the inner and outer walls which reveal the rapid movement of the fluid due to enhanced natural convection at higher value of Ra . Further, as we increase the baffle length, the two vortices are merged to a single vortex near to inner hot wall, while at $Ra = 10^4$, the primary vortex appears near to outer cold wall. Interestingly, at higher Rayleigh number, the variation of flow rate with baffle length is completely reversed as compared to the flow variation at lower value of Ra . For lower Rayleigh number, it has been predicted that the flow rate decreases as baffle length increases. On contrary, at higher value of Ra , increasing the baffle length increases the flow rate. This can be attributed to the fact that with an increase in the value of Ra , the buoyancy effect increases, as a result the fluid flow acquires a supplementary acceleration from the hotter baffle in addition to the heating from the hot wall as well. At higher Rayleigh number, the temperature contours have significantly distorted

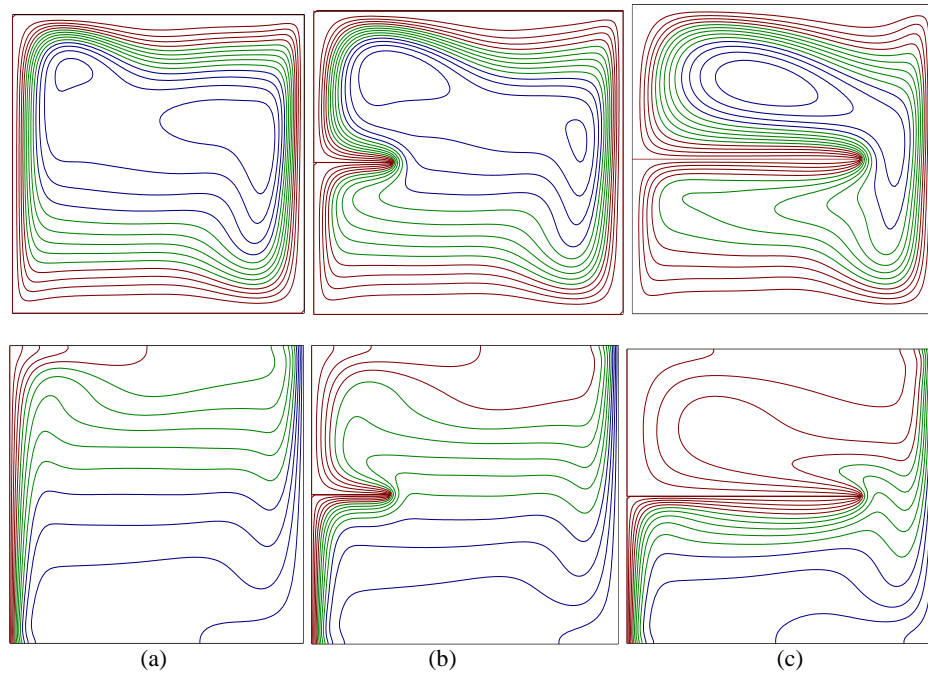


Fig. 4. Effect of baffle length on streamlines (top) and isotherms (bottom) for $L = 0.5$ and $Ra = 10^6$. (a) No baffle, $|\psi_{\max}| = 22.9$, (b) $\varepsilon = 0.25$, $|\psi_{\max}| = 27$ and (c) $\varepsilon = 0.75$, $|\psi_{\max}| = 34.9$.

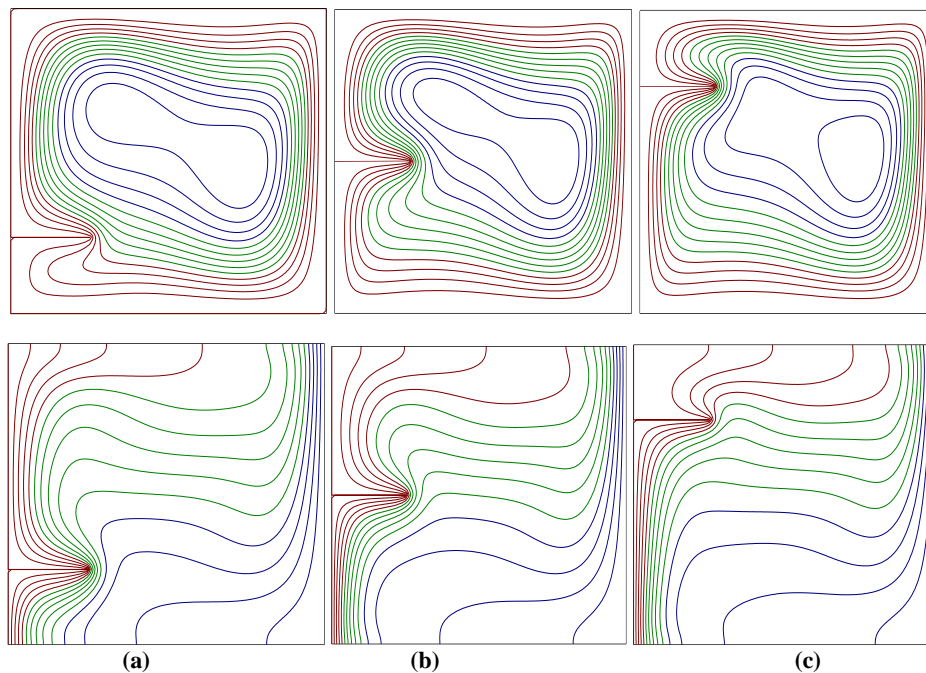


Fig. 5. Effect of baffle position on streamlines (top) and isotherms (bottom) for $\varepsilon = 0.25$ and $Ra = 10^5$. (a) $L = 0.25$, $|\psi_{\max}| = 14.4$, (b) $L = 0.5$, $|\psi_{\max}| = 13.5$, (c) $L = 0.75$, $|\psi_{\max}| = 12.6$.

from the conduction mode, and the isotherms are almost horizontal, which reveals the well established thermally stratified flow in the annular enclosure. Another striking feature at higher Rayleigh number is that the streamlines and isotherms have completely spread over and below the baffle as compared to the lower value of Ra . That is, as the value of Ra increases to 10^6 , the

stagnant flow region above the baffle, exists at $Ra = 10^4$, is occupied by the potential streamlines and isotherms. Further, the densely packed streamlines and isotherms along the vertical walls and baffle indicate the boundary layer formation at these surfaces.

As regards to the location effect of baffle on the

flow and thermal fields, the streamlines and isotherms are exhibited in Fig. 5 for three different locations by fixing $Ra = 10^5$ and $\varepsilon = 0.25$. When the baffle is located near to bottom wall of the annulus, the streamlines are slightly distorted at the bottom and the main vortex is diagonally elongated. However, as the baffle location is moved towards the top adiabatic wall, the main vortex has shifted towards the cold wall, and the magnitude of maximum stream function indicates that the flow rate is also reduced as the baffle position is shifted. An overview of the isotherm contour reveals that the isotherms are not altered to a large extent by the baffle position except around the baffle region. Fig. 6 illustrates the effect of four different combinations of baffle size and position on the streamlines and isotherms at a higher Rayleigh number ($Ra = 10^7$). In particular, we considered the cases of smallest and largest baffles that are placed at lowest and highest locations on the inner wall. At this Rayleigh number, the effect of buoyancy force is dominant and hence the flow rates are higher. As a result, it can be noticed that the strength of convective flow becomes stronger for all baffle lengths and locations as compared to the case of lower Rayleigh number. It is expected that the fluid movement in annulus is blocked by the presence of baffle which in turn reduces the flow circulation and heat transfer rates, and the baffle acts like a barricade to the fluid movement as baffle length increases. However, to our surprise, the flow rate is not declined with baffle length for all baffle locations. It is interesting to note that the flow circulation rate increases with the baffle length, when the baffle is placed near to bottom wall of the annulus. On contrast, when the baffle is placed near to top adiabatic wall, the flow rate reduces as we increase the baffle length. From Fig. 6, for $L = 0.875$, it is evident that the maximum stream function value ($|\psi_{\max}| = 37.3$), has been reduced to ($|\psi_{\max}| = 36.6$), as the baffle length is increased from $\varepsilon=0.25$ to $\varepsilon=0.5$. But, for $L = 0.125$, the maximum stream function value ($|\psi_{\max}| = 43.9$), is increased ($|\psi_{\max}| = 49.4$) as the baffle length increases. We found that the flow circulation rate can be augmented or suppressed by placing the baffle at an appropriate location, and hence it can be concluded that the baffle location is crucial in determining the strength of flow circulation. Further, when a larger baffle is located near to top adiabatic wall, a careful observation of isotherms reveals the formation of stagnant zone above the baffle. These findings are in good agreement with the results predicted by Shi and Khodadadi (2003) for the study of natural convection in a square cavity with a thin fin.

4.2 Effect of Baffle Location and Size on Heat Transfer Rate

In the previous section, the influence of baffle size and location on the flow and thermal fields have been illustrated for wide range of Rayleigh numbers, baffle lengths and locations. However, these interpretations provide only qualitative

information on the convective flow. Hence, the quantitative investigation to understand the effects of Rayleigh number, baffle size and location on the local and average heat transfer rates is performed in this section.

To exhibit the detailed effects of a thin baffle, attached to the inner wall of the annulus, on the local heat transfer rate, the variation of local Nusselt numbers along the inner and outer walls (Nu_L & Nu_R) is illustrated in Fig.7. The local Nusselt numbers are evaluated for various baffle lengths and baffle positions by fixing the Rayleigh number at 10^4 . Along with the variation of local Nusselt number at inner and outer walls for five different locations and three different lengths of the baffle, the variation of Nu_L and Nu_R without baffle is also included for comparison. It is interesting to look through the variations of Nu_L and Nu_R along the inner and outer walls for different baffle lengths and locations. The variation of local Nusselt number along the inner wall (Nu_L) depends on the baffle location to a great extent. In particular, the variation of Nu_L has a jump at the point where baffle is located. It is found that the local heat transfer rate (Nu_L), above and below the baffle, is higher for $L = 0.25$, but fall down rapidly as the baffle position move towards top wall. For the largest baffle length considered in our study ($L = 0.75$), it can be recognized from the figure that the variation of Nu_L is almost flat below the baffle, which indicates a lower heat transfer rate. As the baffle length is increased to its maximum value, the region below or above the baffle has been transformed to a thermally inactive zone, and this tendency strongly depends on the baffle location. Specifically, for $L > 0.5$, the local Nusselt number remains invariant in the region above the baffle, and for $L < 0.5$, Nu_L does not vary in the region below the baffle. Further, a careful observation of the local Nusselt number profiles indicate that the size and location of baffle not only alter the local heat transfer rate at the inner wall, where the baffle is placed, but the local heat transfer rate at the outer wall has also been significantly modified. In general, the local Nusselt number along the inner wall (Nu_L) decreases up to the baffle and then increases. However, Nu_R steadily increases along the outer wall for all baffle sizes and locations. In particular, for the combination of maximum baffle length and position, the value of Nu_R increases significantly along the outer wall. This can be attributed to the fact that when the longer baffle ($\varepsilon = 0.75$) is placed near top wall ($L = 0.875$), the fluid movement in the annulus is restricted to the region below the baffle and is analogous to fluid flow in shallow annular enclosure. As a result, the local Nusselt number at the outer wall is found to be higher at $L = 0.875$ compared to other locations of baffle.

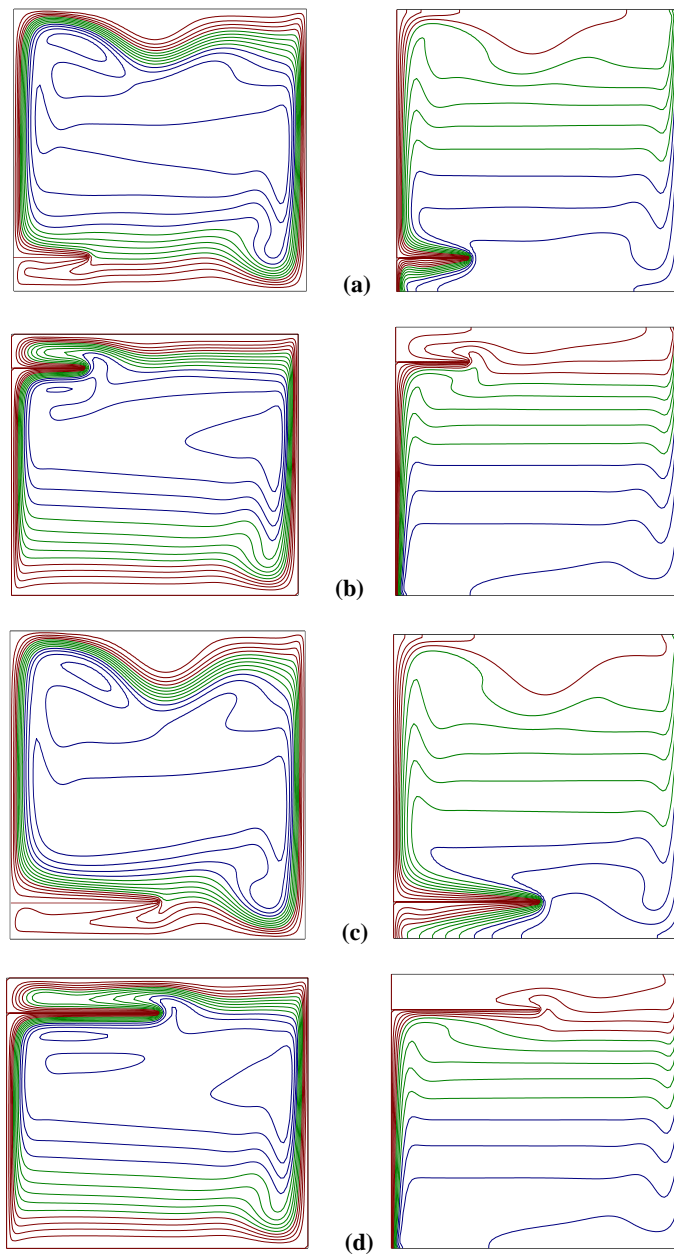


Fig. 6. Streamlines (left) and isotherms (right) for various baffle lengths and positions at $Ra = 10^7$. (a) $|\psi_{\max}| = 43.9$, $(\varepsilon, L) = (0.25, 0.125)$, (b) $|\psi_{\max}| = 37.3$, $(\varepsilon, L) = (0.25, 0.875)$, (c) $|\psi_{\max}| = 49.4$, $(\varepsilon, L) = (0.5, 0.125)$, (d) $|\psi_{\max}| = 36.6$, $(\varepsilon, L) = (0.5, 0.875)$.

To envisage the influence of baffle length on the average heat transfer rate, its effect is illustrated in Fig. 8 by choosing three different baffle lengths ($\varepsilon = 0.25, 0.5$ and 0.75) and the baffles are placed at two different locations $L = 0.25$ and 0.75 . From the figure, it can be observed that the baffle location and length plays a major role in enhancing or suppressing the overall heat transfer rate in the annulus. When the baffle is placed near to bottom wall, it is predicted that the average Nusselt number is higher for a short baffle length compared to longer baffle. As discussed earlier, the presence of baffle enhances the heat transfer rate to an extent that strongly depends on the specific location and

length of the baffle. For higher Rayleigh numbers ($Ra > 10^5$), the average Nusselt number increases sharply compared to lower values of Ra . Furthermore, as the baffle location is shifted near to top wall ($L = 0.75$), the overall heat transfer rate has been decreased significantly for all baffle lengths, and in particular, the variation of \overline{Nu} is almost similar for $\varepsilon = 0.5$ and 0.75 . This indicates the variation of the average Nusselt number is independent of baffle length at $L=0.75$. From these observations, it can be concluded that the overall heat transfer rate in the annulus can be effectively controlled by the proper choice of baffle length and location. The controlling mechanisms of heat

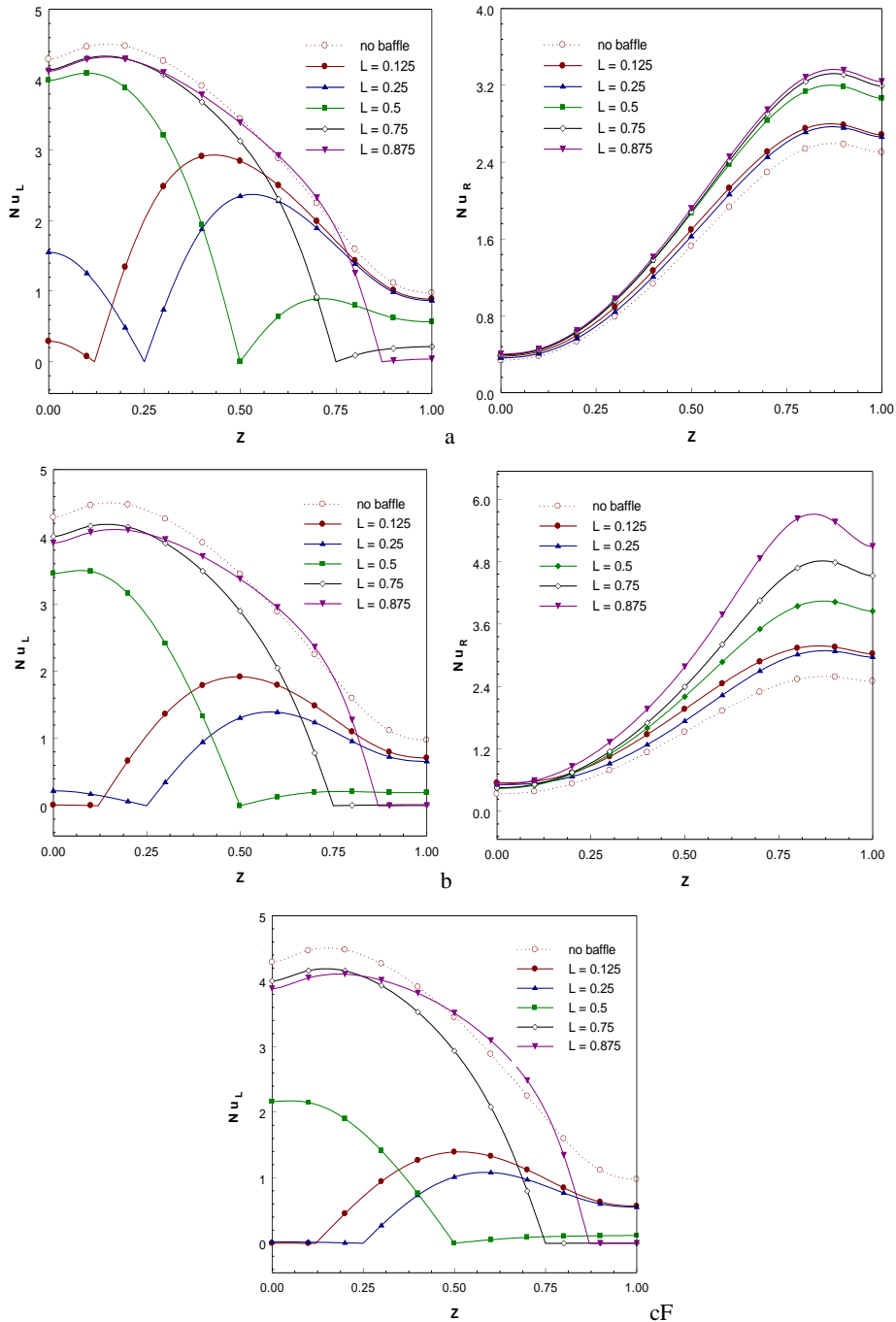


Fig. 7. Variation of local Nusselt number along the inner (left) and outer (right) walls of the annulus for different positions and lengths of baffle at $Ra = 10^4$ (a) $\epsilon = 0.25$, (b) $\epsilon = 0.5$ and (c) $\epsilon = 0.75$.

transfer rate can be achieved with different baffle lengths and locations, since the flow transition in the annulus can be effectively manipulated through different baffle lengths and locations. This flow transition due to baffle lengths and locations makes it possible to either enhance or suppress the heat transfer rate in the annulus.

Figure 9 describes the influence of baffle location on the average heat transfer rate for a fixed baffle length and different values of Ra and L . The Rayleigh number is varied over wide range of values as it is a key parameter in determining the

natural convection flow in the annulus. In the same figure, for the baffle location $L = 0.875$, the average Nusselt number (\overline{Nu}) is determined for the rectangular enclosure ($\lambda = 1$) to compare with the heat transfer rate in the annular enclosure at a similar location. In general, the average heat transfer rate increases with Rayleigh number for any baffle position, since an increase in the Rayleigh number enhances natural convection, and subsequently increases the heat transfer rate. Although the increasing resistance to the fluid due to the baffle decreases the overall heat transfer, it is

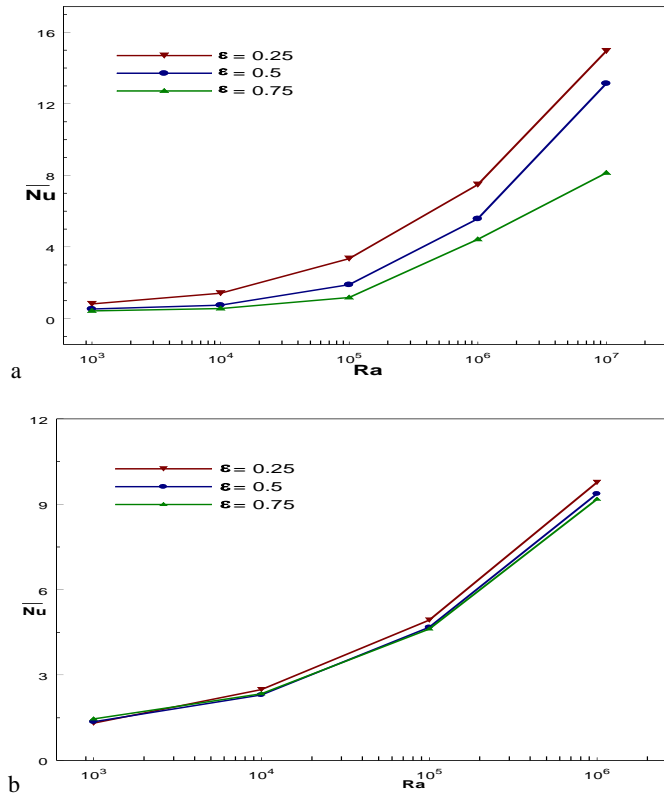


Fig. 8. Effect of baffle length and Rayleigh number on the average Nusselt number for two different baffle positions (a) $L = 0.25$ and (b) $L = 0.75$.

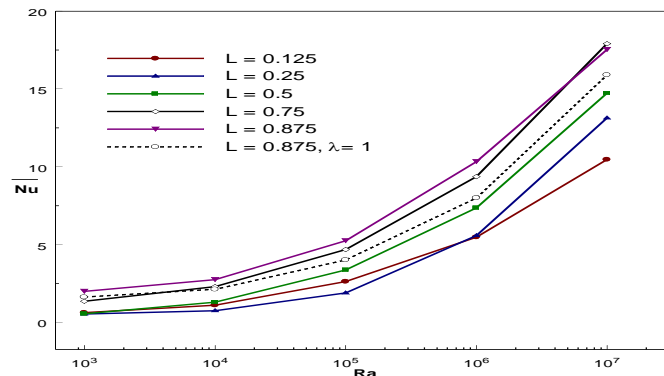


Fig. 9. Effect of baffle position on average Nusselt number for different Rayleigh numbers and $\varepsilon = 0.5$.

not true for all baffle locations. As regards to the influence of baffle location on the heat transfer rate, the average Nusselt number increases with the baffle location. In particular, it has been found that the heat transfer rate attained maximum value when the baffle is positioned at $L = 0.875$. This tendency of heat transfer is anticipated due to the fact that the baffle acts as a barrier to the fluid velocity when it is placed near to bottom wall, where the fluid movement has been originated. When the baffle position is low (near to bottom wall), the fluid circulation is blocked by the baffle and causes a decrease in the fluid velocity. Due to slow moving fluid, major portion of the annulus above the baffle is filled with hot fluid which causes a reduction in heat transfer rate from the hot wall. However, as the baffle position move towards the top wall, the fluid

flow acquires momentum up to the baffle and the portion occupied by the hot fluid above the baffle has also been reduced. As the baffle position move towards the top wall, the total heat transfer surface area in contact with cooler fluid increases, which results in a higher heat transfer rate at these locations. Further, for the baffle location $L = 0.875$, the average Nusselt number is found to be higher at $\lambda = 2$ compared to the value of (\overline{Nu}) at $\lambda = 1$. This indicates that the heat transfer rate in the annulus is higher as compared to the square enclosure.

The effect of curvature in an annular enclosure is an important parameter and its influence on heat transfer rate is investigated for different values of Rayleigh number in Fig. 10. Since the main control parameter in Fig. 10 is the radius ratio, its effect is

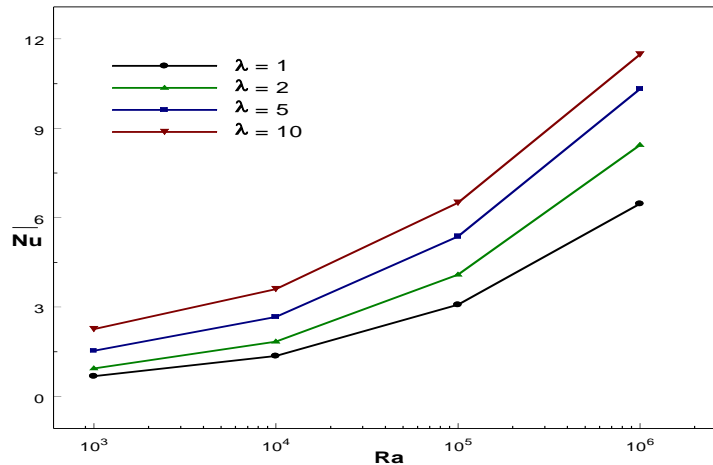


Fig. 10. Effect of radius ratio and Rayleigh number on the average Nusselt number for baffle position $L = 0.5$ and baffle length $\varepsilon = 0.25$.

discussed for four different values $\lambda = 1, 2, 5$ and 10 , and the values of baffle length and location are fixed respectively at $\varepsilon = 0.25$ and $L = 0.5$. In the same figure, heat transfer rate for unit radius ratio ($\lambda = 1$) is also depicted, and the effect of radius ratio on \overline{Nu} is apparent from Fig. 10. As the radius ratio (λ) increases, the percentage of total volume occupied by the hot fluid decreases, and as a result heat transfer rate also increases. Further, the centrosymmetric structure in the flow and thermal fields for $\lambda = 1$ has also been wiped out and the effective sink temperature near the hot wall decreases for $\lambda > 1$. The present results are in full accordance with previous experimental demonstrations and theoretical observations in a vertical annulus without baffle. An overview of the figure reveals that the average heat transfer rate increases with radius ratio for all Rayleigh numbers and hence it can be expected that the annular enclosure stands out better in dissipating higher heat transfer than the square and rectangular enclosures.

5. CONCLUSION

Natural convection in a differentially heated cylindrical annular enclosure has been numerically investigated to explore the influence of a thin baffle on the flow patterns, thermal fields, local and average heat transfer rates. Although the effect of baffle on natural convection heat transfer in finite enclosure has been addressed in the literature, its effect in an annular enclosure has not been addressed, which in our opinion, definitely requires a special attention. The main objective of this study is to illustrate the effect of a thin baffle on convective flow and heat transfer in an annular enclosure, a configuration that has not been examined in the past. Based on the detailed numerical simulations, the following conclusions have been drawn.

The presence of baffle has significant influence on

the flow and thermal fields and the size and location has distinct effects on the flow characteristics and temperature distribution. From the simulations, it was found that the flow circulation rate can be effectively controlled by different baffle lengths and locations. As baffle length is increased, flow circulation is enhanced at high Rayleigh number due to the additional heating from the baffle. However, the flow circulation rate decreases with baffle length at low values of Ra . For $Ra < 10^4$, convection is not strong and hence the presence of baffle resists the fluid movement. As regards to the baffle location on flow circulation rate, we found that the baffle location near top adiabatic wall produces higher flow circulation rate, regardless of baffle lengths. This prediction from our study has been corroborated in the earlier studies on rectangular and triangular enclosures with a baffle attached to one of the active walls. In addition to the flow circulation rates, it has also been observed that the presence of baffle produces stagnant flow region above the baffle at low Rayleigh numbers.

In many industrial applications, such as heat exchangers and electronic equipment cooling, flow and heat transfer rates needs to be effectively controlled or manipulated or channelized and this phenomenon has been successfully achieved in this study by varying the size and location of a thin baffle. By examining the local Nusselt number, it has been found that the heat transfer rate at the outer wall is higher than the inner wall, where the baffle is placed. Further, for larger baffle length, the local heat transfer rates remain flat over and below the baffle based on different baffle locations. From the detailed numerical simulations of the present study, we concluded that the overall heat transfer rate measured by the average Nusselt number can be enhanced by increasing the Rayleigh number or baffle position. However, the heat transfer rate decreases with an increase in baffle length. The heat transfer rates in an annular enclosure with a baffle are higher compared to an identical rectangular enclosure with a baffle. Further, the numerical results reveal that the

overall heat transfer rate increases with radius ratio. An overview of the present results suggests that the flow and heat transfer rates in an annular enclosure can be effectively controlled through proper choice of physical and geometrical parameters.

ACKNOWLEDGEMENTS

The authors MS, BVP and BMRP are respectively grateful to the Managements, R&D Centers and Principals of Presidency University, Bangalore, Saphagiri College of Engineering, Bangalore and SIT, Tumkur and to VTU, Belgaum, India for the support and encouragement. Y. Do was supported by Basic Science Research Program of the Ministry of Education, Science and Technology under Grant No. ~NRF-2013R1A1A2010067. Also, the comments and suggestions from the very competent reviewers are gratefully acknowledged.

REFERENCES

- Al-Abidi, A. A., S. Mat, K. Sopian, M. Y. Sulaiman, and A. T. h. Mohammad (2013). Numerical study of PCM solidification in a triplex tube heat exchanger with internal and external fins. *International Journal of Heat and Mass Transfer* 61, 684–695.
- Ben Nakhi, A and A. J. Chamkha (2006). Effect of length and inclination of a thin fin on natural convection in a square enclosure. *Numerical Heat Transfer, part A* 50, 381-399.
- Ben Nakhi, A. and A. J. Chamkha (2006). Natural convection in inclined partitioned enclosures. *Heat mass Transfer* 42, 311-321.
- Bhattacharya. P. and S. Das (2015). A Study on Steady Natural Convective Heat Transfer inside a Square Cavity for Different Values of Rayleigh and Nusselt Numbers. *Journal of Applied Fluid Mechanics* 8, 635- 640.
- Bilgen, E. (2002). Natural convection in enclosures with partial partitions. *Renewable Energy* 26, 257-270.
- Bilge, E. (2005). Natural convection in cavities with a thin fin on the hot wall. *International Journal of Heat and Mass Transfer* 48, 3493-3505.
- Bose, P. K., D. Sen, R. Panua and A. K. Das (2013). Numerical analysis of laminar natural convection in a quadrantal cavity with a solid adiabatic fin attached to the hot vertical wall. *Journal of Applied Fluid Mechanics* 6, 501-510.
- Changzheng, S., B. Yua, H. F. Oztop, Y. Wang and J. Weic (2011). Control of mixed convection in lid-driven enclosures using conductive triangular fins. *Int. Journal of Heat and Mass Transfer* 31, 894-909.
- Kumar, A. and A. K. Singh (2013). Effect of induced magnetic field on natural convection in vertical concentric annuli heated/cooled asymmetrically. *Journal of Applied Fluid Mechanics* 6, 15-26.
- Liu, Y., C. Lei and J. C. Patterson (2014). Natural convection in a differentially heated cavity with two horizontal adiabatic fins on the sidewalls. *International Journal of Heat and Mass Transfer* 72, 23-36.
- Moukalled, F. and M. Darwish (2007). Buoyancy induced heat transfer in a trapezoidal enclosure with offset baffles. *Numerical Heat Transfer, Part A* 52, 337-355.
- Nag, A., A. Sarkar and V. M. K. Sastri (1994). Effect of thick horizontal partial partition attached to one of the active walls of a differentially heated square cavity. *Numerical Heat Transfer, part A* 25, 611-625.
- Ostrach, S. (1988). Natural convection in enclosures. *ASME J. Heat Transfer* 110, 1175–1190.
- Oztop, H. F., I. Dagtekin and A. Bahloul (2004). Comparison of position of a heated thin plate located in a cavity for natural convection. *International Communications in Heat and Mass Transfer* 31, 121-132.
- Patil, M., P. G. Hegde and K. N. Seetharamu (2013). Effects of radiation and cold wall temperature boundary conditions on natural convection in a vertical annular porous medium. *Journal of Applied Fluid Mechanics* 6(2), 177-189.
- Sankar, M., B. Jang and Y. Do (2014). Numerical study of non-Darcy natural convection from two discrete heat sources in a vertical annulus. *Journal of Porous Media* 17, 373–390.
- Sankar, M., B. Kim, J. M. Lopez and Y. Do (2012). Thermosolutal convection from a discrete heat and solute source in a vertical porous annulus. *Int. Journal of Heat and Mass Transfer* 55, 4116-4128.
- Sankar, M., J. Park, D. Kim and Y. Do (2013). Numerical study of natural convection in a vertical porous annulus with an internal heat source: effect of discrete heating. *Numerical Heat Transfer, Part A: Applications* 63, 687-712.
- Sankar, M., M. Venkatachalappa and Y. Do (2011). Effect of magnetic field on the buoyancy and thermocapillary driven convection of an electrically conducting fluid in an annular enclosure. *Int. J. Heat Fluid Flow* 32, 402-412.
- Shi, X. and J. M. Khodadadi (2003). Laminar natural convection heat transfer in differentially heated square cavity due to a thin fin on the hot wall. *Journal of Heat Transfer* 125, 624-634.
- Sun, Y. S. and A. F. Emery (1997). Effects of wall conduction, internal heat sources and an internal baffle on natural convection heat transfer in a rectangular enclosure. *Int. J. Heat Mass Transfer* 40, 915-929.

- Tandiroglu, A. (2006). Effect of flow geometry parameters on transient heat transfer for turbulent flow in a circular tube with baffle inserts. *International Journal of Heat and Mass Transfer* 49, 1559–1567.
- Tasnim, S. H. and M. R. Collins (2004). Numerical analysis of heat transfer in a square cavity with a baffle on the hot wall. *International Communications in Heat and Mass Transfer* 31, 639-650.
- Tasnim, S. H. and M. R. Collins (2005). Suppressing natural convection in a differentially heated square cavity with an arc shaped baffle. *Int. Communications in Heat and Mass Transfer* 32, 94–106.
- Varol, Y. and H. F. Oztop (2009). Control of buoyancy-induced temperature and flow fields with an embedded adiabatic thin plate in porous triangular cavities. *Applied Thermal Engineering* 29, 558–566.